

Identification of differentially expressed proteins in the gastric mucosal atypical hyperplasia tissue microenvironment

HE-LIANG ZHANG^{1,2}, CHONG-YUAN LIU¹, WEI MA¹, LIN HUANG³,
CHANG-JIAN LI⁴, CHENG-SONG LI⁴ and ZHI-WEI ZHANG¹

¹Key Laboratory of Cancer Cellular and Molecular Pathology, Cancer Research Institute of Medical College, University of South China, Hengyang, Hunan 421001; ²Medical Company, Troops 66028 of People's Liberation Army, Chengde, Hebei 067000; ³Department of Pediatrics, Shaoyang Medical School, Shaoyang, Hunan 422000; ⁴Clinical Medicine Undergraduate Program, Medical College, University of South China, Hengyang, Hunan 421001, P.R. China

Received October 15, 2017; Accepted April 5, 2018

DOI: 10.3892/ol.2018.8941

Abstract. In the present study, the interaction of proteins in the microenvironment of gastric mucosal atypical hyperplasia was analyzed. The stromata of normal gastric mucosa (NGM) and gastric mucosal atypical hyperplasia (GMAH) tissues were purified with laser capture microdissection (LCM). The differentially expressed GMAH proteins of the NGM and GMAH tissues were identified by quantitative proteomic techniques with isotope labeling. The cross-talk between differentially expressed proteins in NGM and GMAH tissues was then analyzed by bioinformatics. There were 165 differentially expressed proteins identified from the stromata of NGM and GMAH tissues. Among them, 99 proteins were upregulated and 66 were downregulated in GMAH tissue. The present study demonstrated that these proteins in gastric mucosal atypical hyperplasia were involved in cancer-associated signaling pathways, including the p53, mitogen-activated protein kinase (MAPK), cell cycle and apoptosis signaling pathways, and were involved in cellular growth, cellular proliferation, apoptosis and the humoral immune response. The results of the present study suggest that the 165 differentially expressed proteins, including S100 calcium-binding protein A6 (S100A6) and superoxide dismutase 3 (SOD3) in the microenvironment of gastric mucosal atypical hyperplasia, are involved in the p53, MAPK, cell cycle and apoptosis signaling pathways, and serve a function in the pathogenesis of gastric cancer.

Introduction

Gastric carcinoma (GC), a serious threat to human health, is one of the most common malignancies in China, and its incidence and deaths rank first in the digestive system in 2015 (1). The occurrence of GC involves a complex pathological process associated with polygenic interactions and multi-phase evolution (2). The majority of patients experience the typical stages of normal gastric mucosa, chronic atrophic gastritis, precancerous lesions (atypical hyperplasia of gastric mucosa and intestinal metaplasia), early stages of gastric cancer, and advanced stage of disease (3). However, at present, the molecular mechanisms underlying the occurrence of GC remain unclear.

The cross-talk that exists between tumor cells and the microenvironment serves an important function in the occurrence and development of tumors (4). Tumor cells adapt to their microenvironment and exhibit corresponding biological characteristics. The tumor microenvironment refers to the internal environment in which the tumor grows, which is primarily composed of various interstitial cells, blood vessels, nerves, interstitial fluid and a small number of leucocytes (5). Tumor cells are able to induce mesenchymal cells to produce a variety of cytokines and growth factors that promote tumorigenesis and development (6). According to previous studies (7), it is possible to target the formation mechanism of the tumor microenvironment in order to prevent the proliferation and metastasis of tumor cells. Knowledge of the interaction between the microenvironment and tumor cells is expected to provide a rich theoretical basis for the treatment of tumors. The aim of the present study was to elucidate the molecular mechanisms underlying the occurrence of GC by analyzing the protein interactions in gastric mucosal atypical hyperplasia.

Materials and methods

Tissue samples. Matching specimens, including 20 cases of normal gastric mucosa (NGM) tissue and gastric mucosa atypical hyperplasia (GMAH) tissue, were collected from

Correspondence to: Dr Zhi-Wei Zhang, Key Laboratory of Cancer Cellular and Molecular Pathology, Cancer Research Institute of Medical College, University of South China, 28 Changsheng Road, Hengyang, Hunan 421001, P.R. China
E-mail: nhdxzzw@qq.com

Key words: gastric mucosal atypical hyperplasia, microenvironment, protein expression

The First Affiliated Hospital of University of South China between September 2016 and June 2017. The Cancer Research Institute of University of South China and The First Affiliated Hospital of University of South China are cooperative relations. Researchers from Cancer Research Institute are permitted to travel to the hospital and collect specimens with the permission of the medical ethics committee of University of South China. Specimens were collected from the stomach within 5 min of resection, and the gastric mucosal surface was washed with physiological saline prior to and following the incision. The samples were immediately frozen in liquid nitrogen and stored at -80°C . Table I presented the clinical data including tumor stage determined by the eighth edition AJCC cancer staging manual (8) of 20 patients with GC. Two senior professional pathologists from Cancer Research Institute of University of South China were asked to independently diagnose the collected tissue samples without knowing any clinical or pathological data.

Ethics statement. The human GC tissue samples were collected from The First Affiliated Hospital of University of South China according to the institutional and governmental guidelines. All patients involved in the present study provided written informed consent, and the present study was approved by the medical ethics committee of University of South China (Hengyang, China).

Preparation and staining of frozen sections. The tissue samples were removed from liquid nitrogen and placed on a cryostat device carrier (Leica Biosystems GmbH, Wetzlar, Germany). Following the addition of optimal cutting temperature compound (OCT) embedding agent (Leica Microsystems GmbH), the samples were frozen at -25°C for 20 min. Next, the samples were immobilized to the platform of the cryostat device, and frozen sections were made at a thickness of $8\text{ }\mu\text{m}$. The frozen sections were affixed to film slides (Leica Microsystems GmbH) pretreated with ultraviolet (UV) light. Finally, the slides were fixed with 75% ethanol at 4°C for 60 sec, stained with 0.5% methyl green (Sigma-Aldrich; Merck KGaA, Darmstadt, Germany) at 4°C for 30 sec and discolored with 95% ethanol at 4°C for 5 sec.

Laser capture microdissection (LCM). The frozen tissue sections stained with methyl green were placed on an LCM apparatus (Leica LMD6, Leica Microsystems GmbH) platform. The target tissue was outlined on the display, and the laser automatically cut the target tissue in the slice. Dissolved one tablet of protease inhibitor cocktail tablets (Roche Diagnostics, Basel, Switzerland) in 50 ml ultrapure water to prepare 5% working solutions. The tissues were collected in a tube containing 2–3 μl protease inhibitor working solutions and were frozen at -80°C for later use.

Protein extraction and isobaric tags for relative and absolute quantitation (iTRAQ) isotope labeling. The mesenchyma of the NGM and GMAH tissues were extracted using a lysis buffer (10 mM PMSF, 65 mM dithiothreitol, 7 M urea and 2 M thiourea) (GE Healthcare Life Sciences, Little Chalfont, UK) and centrifuged at 4°C , $12,000\times g$ for 30 min. The supernatant included the total proteins of the NGM and GMAH

mesenchyma. The total proteins were extracted and quantified using a bicinchonic acid protein assay kit (Beyotime Institute of Biotechnology, Shanghai, China), according to the manufacturer's protocol. The total proteins of the NGM mesenchyma were labeled with iTRAQ reagent 114; total proteins of the GMAH mesenchyma were labeled with iTRAQ reagent 118 (both Applied Biosystems; Thermo Fisher Scientific, Inc., Waltham, MA, USA) according to the manufacturer's protocol. A total of 100 μl ultrapure water was used to end the reaction. All protein samples were homogenized and lyophilized, and then the samples were dissolved in deionized water containing 0.1% formic acid (FA; Tedia Company, Fairfield, OH, USA). The marked samples were eluted twice with Sep-Pak C_{18} 1 cc Vac cartridges (Waters Corporation, Milford, MA, USA) with deionized water containing 0.1% FA and then once with 50% acetonitrile (ACN) (Thermo Fisher Scientific, Inc.) containing 0.1% FA. The cleaning solution was collected and lyophilized.

Identification of differentially expressed proteins. The samples marked with iTRAQ were dissolved in 1 ml strong cation-exchange (SCX) buffer [25% (v/v) ACN and 10 mM KH_2PO_4 , pH 2.6] for SCX separation. The two samples containing mesenchymal proteins of NGM and GMAH were mixed and loaded into a polysulfoethyl column and segregated using a 20AD high performance liquid chromatography (HPLC) system (Shimadzu Corporation, Kyoto, Japan) with the following conditions: i) 10 mM KH_2PO_4 and 25% ACN, pH 2.6; ii) 10 mM KH_2PO_4 , 350 mM KCl and 25% ACN, pH 2.6. The following settings were used: UV detection wavelength: 214/280 nm; flow rate: 200 $\mu\text{l}/\text{min}$ for 60 min; salt gradient: from 5% i) at 5 min to 25% ii) at 40 min. Next, the products were concentrated by vacuum centrifugation for reverse-phase HPLC-mass spectrometry (MS) analysis. The samples were dissolved in 50 μl 5% ACN containing 0.1% FA and were loaded into a Zorbax 300SB- C_{18} column (Agilent Technologies, Inc., Santa Clara, CA, USA). The conditions were as follows: i) 5% ACN, 0.1% FA; ii) 95% ACN, 0.1% FA. Flow rate: 300 nl/min for 90 min. Salt gradient: from 5% i) at 5 min to 35% ii) at 70 min. The data were analyzed using QSTAR-XL (Applied Biosystems; Thermo Fisher Scientific, Inc.) and tandem MS (MS/MS). Finally, the IPI human database (version 3.45; URL: <http://www.ebi.ac.uk/IPI>) was searched for protein information, and the confidence level was set to be $>95\%$, and the ion peak areas of m/z 114 and 118 were integrated to perform relative quantitative analysis of proteins.

Western blot analysis. The total NGM and GMAH mesenchymal proteins were mixed with 5X loading buffer (Beyotime Institute of Biotechnology) and boiled for 5 min. The proteins had been quantified using a bicinchonic acid protein assay kit (Beyotime Institute of Biotechnology). Next, the samples were separated using 10% gradient SDS-PAGE gels at 30 μg per lane and transferred onto PVDF membranes (Merck KGaA). The membranes were blotted with 5% fat-free milk suspended in TBST at room temperature for 1 h, incubated at 4°C overnight with S100 calcium-binding protein A6 (S100A6) antibody (1:1,000) (sc-53950; Santa Cruz Biotechnology, Inc., Dallas, TX, USA) and superoxide dismutase 3 (SOD3) antibody (1:1,000) (sc-58427; Santa Cruz Biotechnology, Inc.), washed

Table I. Clinicopathological features of patients with gastric cancer.

No.	Sex	Age, years	Differentiation	Tumor stage (8)	Date of collection
1	Male	49	Moderate	II	September 2016
2	Female	64	Poor	IV	September 2016
3	Female	69	Poor	IV	September 2016
4	Male	62	Poor	II	October 2016
5	Male	44	Moderate	II	October 2016
6	Male	60	Poor	II	November 2016
7	Male	53	Poor	II	November 2016
8	Female	40	Poor	III	November 2016
9	Male	67	Poor	II	December 2016
10	Female	81	Poor	II	December 2016
11	Female	47	High	II	January 2017
12	Male	63	Poor	II	February 2017
13	Male	52	Poor	IV	March 2017
14	Male	46	Moderate	II	March 2017
15	Male	51	Poor	II	March 2017
16	Male	60	Moderate	II	March 2017
17	Female	66	Poor	III	April 2017
18	Male	67	Poor	II	April 2017
19	Female	68	Poor	II	May 2017
20	Female	62	Poor	III	June 2017

and then incubated with goat anti-mouse IgG-HRP (1:2,000) (sc-2005; Santa Cruz Biotechnology, Inc.) at room temperature for 2 h. Detection of immunoreactivity was achieved using enhanced chemiluminescence (GE Healthcare Life Sciences).

Immunohistochemistry. The present study used S-P immunohistochemical staining kits (MXB Company, Fujian Province, China; URL: <http://www.maxim.com.cn/>). The NGM and GMAH tissues were fixed with 10% formalin and embedded in paraffin. The expression of S100A6 and SOD3 proteins were detected according to the manufacturer's protocol. Briefly, 4- μ m-thick sections were prepared and mounted on poly-L-lysine-coated glass slides, air-dried, deparaffinized with xylene and rehydrated in a descending ethanol series. Following microwave treatment for 20 min, endogenous peroxidase activity was suppressed using 0.3% hydrogen peroxide. The sections were treated with 5% normal goat serum (SL038) (Solarbio Life Sciences, Tongzhou Dist. Beijing, China) at room temperature for 15 min to block non-specific binding. The sections were incubated with anti-S100A6 (1:100) or anti-SOD3 (1:100) antibody overnight at 4°C, and then incubated with goat anti-mouse IgG-FITC (1:200) (sc-2010; Santa Cruz Biotechnology, Inc.) at room temperature for 60 min followed by horseradish peroxidase-labeled streptavidin for 5 min at room temperature. The sections were counterstained with 0.1% hematoxylin at room temperature for 30 sec. The tissue staining was observed under a light microscope at a magnification of x40. The final immunoreactive score was based on protein staining intensity and the percentage of positive cells. Staining intensity was defined as 1 (negative), 2 (yellow) and 3 (brown). The percentage of positive cells was defined as 1 (<10% positive

cells), 2 (11-50% positive cells) and 3 (>50% positive cells). The final immunoreactive score was calculated as: Staining intensity x percentage of positive cells. The classification of the final score was defined as - (score 1), + (score 2-4) and +++ (score >4).

Protein signaling pathways and interaction analysis. Visant software (version 3.91; URL: <http://visant.bu.edu>) was used to analyze the interactions between proteins. Additionally, the network of direct interactions between proteins was analyzed. The Clue Gene Ontology (GO), Kyoto Encyclopedia of Genes and Genomes (KEGG) analysis of protein signaling pathways was performed using Cytoscape software (version 2.8.2; URL: <http://www.cytoscape.org>). GO_BP, GO_CC and GO_MF analyses were executed with David Functional Annotation (URL: <http://david.abcc.ncifcrf.gov>).

Statistical analysis. The data are reported as the mean \pm standard deviation. Statistical analysis was performed using SPSS statistical package (version 18.0; SPSS, Inc., Chicago, IL, USA) as follows: Comparison between individual subgroups was performed using the Mann-Whitney U test, and correlation analysis between groups was performed using Spearman's rank correlation test. $P < 0.05$ was considered to indicate a statistically significant difference.

Results

Purified mesenchyma of NGM and GMAH tissues. The NGM and GMAH tissues were obtained from fresh specimens of GC following surgical resection, and all tissues were confirmed by pathology. The mesenchyma of NGM and GMAH tissues were

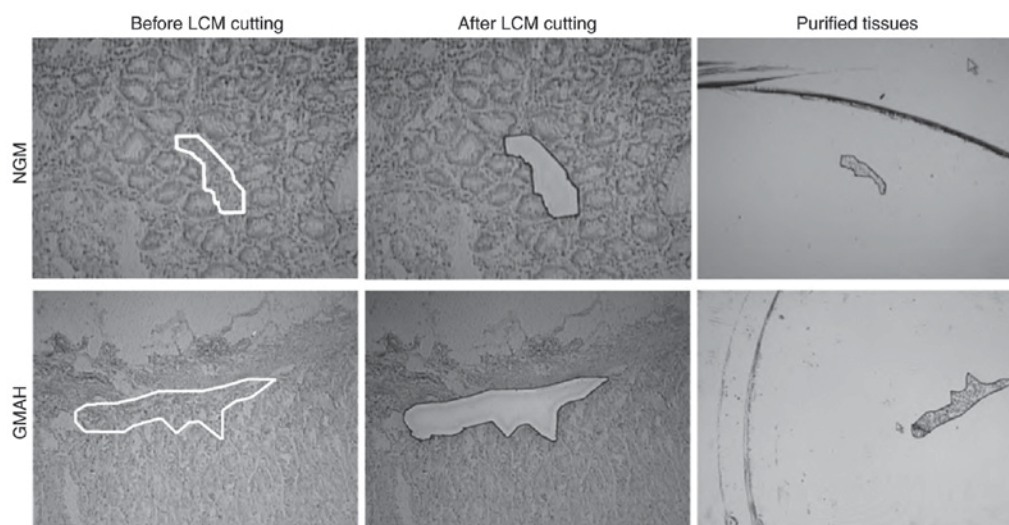


Figure 1. Purification of mesenchyma of NGM and GMAH tissues by LCM. The purified mesenchyma of NGM and GMAH tissues prior to and following LCM are indicated in the area surrounded by the closed line at a magnification of $\times 10$. NGM, normal gastric mucosa; GMAH, gastric mucosal atypical hyperplasia; LCM, laser-capture microdissection.

purified by LCM (Fig. 1). The purity of objective groups was $>95\%$.

Identification of differentially expressed proteins. The NGM and GMAH mesenchyma proteins were divided into solutions and marked using different isotopic iTRAQ. Next, the NGM and GMAH proteins were separated using a 20AD HPLC system and identified using QSTAR-XL MS/MS. A total of 165 differentially expressed proteins between the NGM and GMAH mesenchyma were identified (Table II). The G/N value (NGM/GMAH tissue) was determined as the mean protein expression level. In total, 99 proteins ($G/N > 1.5$) were identified to be upregulated and 66 proteins ($G/N < 0.667$) were identified to be downregulated in the GMAH mesenchyma. The expression levels of the S100A6 and SOD3 proteins were different in the mesenchyma of the NGM and GMAH tissues, and were associated with tumorigenesis in previous studies (9,10). Fig. 2 presents the MS results and the quantification of the S100A6 (Fig. 2A) and SOD3 proteins (Fig. 2B).

S100A6 is upregulated and SOD3 is downregulated in GMAH mesenchymal tissue. The 20 samples of NGM and GMAH tissues were collected and purified. Next, the tissues were sectioned. The expression levels of the S100A6 and SOD3 proteins in NGM and GMAH mesenchyma were detected using western blotting and immunohistochemistry. The result of western blotting indicated that the S100A6 protein was upregulated, but that the SOD3 protein was significantly downregulated in the GMAH mesenchyma when compared with the NGM tissue ($P < 0.01$; Fig. 3A). Immunohistochemistry analysis demonstrated that S100A6 and SOD3 proteins were expressed in the mesenchyma of NGM and GMAH tissues; however, the staining intensity and expression levels of the S100A6 protein in the GMAH tissue were increased compared with those in the NGM tissue. The expression of the SOD3 protein was the opposite (Fig. 3B and C). Therefore, the S100A6 and SOD3 expression levels were significantly different between the NGM and GMAH tissues ($P < 0.05$; Table III). These results

were consistent with the results of quantitative proteomics in the present study (Table II).

Interaction of differentially expressed proteins and relevant signaling pathways analysis. The interaction between 165 differentially expressed proteins in GMAH were analyzed using Visant software. It was identified that 140 proteins acted as network nodes and interacted with each other. The results of KEGG signal pathway analysis demonstrated that the 165 proteins were involved in a number of tumor signaling pathways, including the p53, mitogen-activated protein kinase (MAPK), cell cycle, and apoptosis signaling pathways (Fig. 4). Next, the biological functions of the 165 proteins were analyzed with the David tool, which indicated that the proteins were involved in cell growth, proliferation, apoptosis and the humoral immune response (results not shown).

Discussion

The microenvironment is composed of stromal cells, immune cells and cytokines, and the tumor microenvironment has been proven to determine the biological behavior of tumor cells (11,12). It is hypothesized that the interactions of protease, cytokines and receptors in the tumor microenvironment affect the osmotic pressure and metabolism of the tumor, which may result in immune escape and neoplasia (13,14). It is important to monitor cell behavior and prevent cancer by understanding changes in the microenvironment, which serve important functions in tumor occurrence and development (4). In the present study, 165 proteins that were differentially expressed between the NGM and GMAH tissue microenvironments were screened. These proteins were demonstrated to be involved in signaling pathways associated with cancer, including the MAPK, VEGF and p53 signaling pathways, suggesting that these proteins may regulate cell growth, proliferation, apoptosis and the humoral immune response. However, the interaction network should be further characterized in follow-up studies. In the present study, the

Table II. Differentially expressed proteins between the NGM and GMAH mesenchyma.

No.	Accession no.	Protein name	GMAH vs. NGM
1	IPI00872780.1	ANXA4, annexin A4	↑1.5704
2	IPI00027230.3	HSP90B1, endoplasmic precursor	↑1.5704
3	IPI00024920.1	ATP5D, ATP synthase subunit δ	↑1.5704
4	IPI00013508.5	ACTN1, α -actinin-1	↑1.5848
5	IPI00216135.1	TPM1, isoform 3 of tropomyosin α -1 chain	↑1.5995
6	IPI00788802.1	TKT, transketolase variant	↑1.6292
7	IPI00647915.1	TAGLN2, 24 kDa protein	↑1.6292
8	IPI00025874.2	RPN1	↑1.6750
9	IPI00020599.1	CALR, calreticulin precursor	↑1.7062
10	IPI00219219.3	LGALS1, galectin-1	↑1.7379
11	IPI00218918.5	ANXA1, annexin A1	↑1.7379
12	IPI00218733.6	SOD1, superoxide dismutase	↑1.7864
13	IPI00010796.1	P4HB, protein disulfide-isomerase precursor	↑1.7864
14	IPI00414283.5	FN1, fibronectin 1 isoform 4 preproprotein	↑1.8198
15	IPI00298547.3	PARK7, protein DJ-1	↑1.8198
16	IPI00794402.1	ARHGDI1, 28 kDa protein	↑1.8365
17	IPI00219446.5	PEBP1, phosphatidylethanolamine-binding protein 1	↑1.8879
18	IPI00553177.1	SERPINA1	↑1.9771
19	IPI00029623.1	PSMA6, proteasome subunit α type-6	↑1.9952
20	IPI00026314.1	GSN, isoform 1 of gelsolin precursor	↑2.0137
21	IPI00479186.5	PKM2	↑2.0700
22	IPI00033494.3	MRLC2, myosin regulatory light chain	↑2.0700
23	IPI00418471.6	VIM, vimentin	↑2.2492
24	IPI00169383.3	PGK1, phosphoglycerate kinase 1	↑2.2492
25	IPI00396321.1	LRRC59, leucine-rich repeat-containing protein 59	↑2.2696
26	IPI00027947.6	CTRL, chymotrypsin-like protease	↑2.2696
27	IPI00884105.1	LAMP1	↑2.3337
28	IPI00789605.1	MYL6	↑2.3770
29	IPI00219018.7	GAPDH, glyceraldehyde-3-phosphate dehydrogenase	↑2.3770
30	IPI00021405.3	LMNA, isoform A of lamin-A/C	↑2.3770
31	IPI00654755.3	HBB, hemoglobin subunit β	↑2.3987
32	IPI00024284.4	HSPG2	↑2.4661
33	IPI00020987.1	PRELP, prolargin precursor	↑2.4888
34	IPI00871843.1	TGM2, 81 kDa protein	↑2.5349
35	IPI00418169.3	ANXA2, annexin A2 isoform 1	↑2.5349
36	IPI00291136.4	COL6A1, collagen α -1(VI) chain	↑2.5349
37	IPI00009771.6	LMNB2, lamin-B2	↑2.5349
38	IPI00742225.1	LOC646483, DNA-binding protein TAXREB107 isoform 1	↑2.5589
39	IPI00297084.7	DDOST	↑2.6062
40	IPI00216138.6	TAGLN, transgelin	↑2.6546
41	IPI00025252.1	PDIA3, protein disulfide-isomerase A3	↑2.6788
42	IPI00414676.6	HSP90AB1, heat-shock protein HSP 90- β	↑2.8843
43	IPI00009904.1	PDIA4, protein disulfide-isomerase A4	↑2.8843
44	IPI00382696.1	FLNB, isoform 2 of filamin-B	↑2.9104
45	IPI00022200.2	COL6A3, α 3 type VI collagen isoform 1	↑2.9922
46	IPI00479145.2	KRT19, type I cytoskeletal 19	↑3.0202
47	IPI00792191.1	GATM, glycine amidinotransferase	↑3.0479
48	IPI00872814.1	Uncharacterized protein MSN (fragment)	↑3.1328
49	IPI00008274.7	CAP1, adenylate cyclase-associated protein 1	↑3.1328
50	IPI00887241.1	LOC650788, 40S ribosomal protein S28	↑3.2206
51	IPI00829626.1	IGL@ protein	↑3.2206
52	IPI00220278.5	MYL9, myosin regulatory light chain 2	↑3.2206

Table II. Continued.

No.	Accession no.	Protein name	GMAH vs. NGM
53	IPI00021766.5	RTN4, isoform 1 of reticulon-4	↑3.2510
54	IPI00871932.1	SPTBN1, 276 kDa protein	↑3.3422
55	IPI00465431.7	LGALS3, galectin-3	↑3.3422
56	IPI00333541.6	FLNA, filamin-A	↑3.4674
57	IPI00221226.7	ANXA6, annexin A6	↑3.5323
58	IPI00025465.1	OGN, mimecan precursor	↑3.5323
59	IPI00013296.3	RPS18	↑3.5651
60	IPI00299145.9	KRT6C, type II cytoskeletal 6C	↑3.7665
61	IPI00515087.2	CTRB2, chymotrypsinogen B2	↑4.0933
62	IPI00450768.7	KRT17, type I cytoskeletal 17	↑4.0933
63	IPI00745872.2	ALB, isoform 1 of serum albumin precursor	↑4.2070
64	IPI00218914.5	ALDH1A1, retinal dehydrogenase 1	↑4.8309
65	IPI00027350.3	PRDX2, peroxiredoxin-2	↑4.8309
66	IPI00000874.1	PRDX1, peroxiredoxin-1	↑4.8309
67	IPI00887678.1	LOC654188, peptidylprolyl isomerase A-like	↑5.1520
68	IPI00848226.1	GNB2L1	↑5.3937
69	IPI00883857.1	HNRNPU	↑5.4945
70	IPI00744153.2	Uncharacterized protein GCG	↑5.8072
71	IPI00020986.2	LUM, lumican precursor	↑5.8617
72	IPI00010471.5	LCP1, plastin-2	↑5.9172
73	IPI00028030.3	COMP, cartilage oligomeric matrix protein	↑6.1958
74	IPI00220271.3	AKR1A1, alcohol dehydrogenase	↑6.6050
75	IPI00000690.1	AIFM1, isoform 1 of apoptosis-inducing factor 1	↑6.6050
76	IPI00296099.6	THBS1, thrombospondin-1 precursor	↑6.7935
77	IPI00798430.1	TF, transferrin variant	↑7.0472
78	IPI00410241.2	POSTN, periostin, osteoblast specific factor	↑7.1124
79	IPI00646304.4	PPIB, peptidylprolyl isomerase B precursor	↑7.3801
80	IPI00022391.1	APCS, serum amyloid P-component precursor	↑7.3801
81	IPI00021263.3	YWHAZ, 14-3-3 protein ζ/δ	↑7.3801
82	IPI00607708.3	LDHA, isoform 2 of L-lactate dehydrogenase A chain	↑8.3963
83	IPI00749250.2	ACTR2 45 kDa protein	↑8.7108
84	IPI00004457.3	AOC3, membrane copper amine oxidase	↑10.2775
85	IPI00027463.1	S100A6, protein S100 A6	↑10.3734
86	IPI00215719.6	RPL18, 60S ribosomal protein L18	↑10.7643
87	IPI00014361.1	TSTA3, GDP-L-fucose synthetase	↑11.3766
88	IPI00012750.3	RPS25, 40S ribosomal protein S25	↑12.2399
89	IPI00010414.4	PDLIM1, PDZ and LIM domain protein 1	↑12.2399
90	IPI00744375.1	HLA-C	↑12.7065
91	IPI00399007.5	IGHG2	↑13.5501
92	IPI00291006.1	MDH2	↑14.4509
93	IPI00807428.1	Putative uncharacterized protein	↑16.8919
94	IPI00738499.2	FTL, ferritin light chain	↑20.8768
95	IPI00215965.2	HNRNPA1	↑26.5252
96	IPI00790262.1	TTLL3	↑27.0270
97	IPI00550991.3	SERPINA3	↑32.4675
98	IPI00015911.1	DLD, dihydrolipoyl dehydrogenase	↑38.7597
99	IPI00060715.1	KCTD12	↑39.0625
100	IPI00465084.6	DES, desmin	↓0.0406
101	IPI00396378.3	HNRNPA2B1	↓0.0855
102	IPI00514669.1	SH3BGRL	↓0.0991
103	IPI00027827.2	SOD3	↓0.1057
104	IPI00025476.1	AMY1B, pancreatic α-amylase precursor	↓0.1086

Table II. Continued.

No.	Accession no.	Protein name	GMAH vs. NGM
105	IPI00473011.3	HBD, hemoglobin subunit δ	\downarrow 0.1127
106	IPI00847342.1	KRT7, keratin 7	\downarrow 0.1148
107	IPI00877792.1	FGG, 50 kDa protein	\downarrow 0.1259
108	IPI00815665.1	PRSS1, PRSS1 protein	\downarrow 0.1259
109	IPI00011654.2	TUBB, tubulin β chain	\downarrow 0.1306
110	IPI00021885.1	FGA, isoform 1 of fibrinogen α chain precursor	\downarrow 0.1318
111	IPI00009634.1	SQRDL	\downarrow 0.1803
112	IPI00478003.1	A2M, α_2 -macroglobulin precursor	\downarrow 0.2014
113	IPI00867509.1	CORO1C, coronin-1C_i3 protein	\downarrow 0.2291
114	IPI00642455.2	THBS2, thrombospondin 2	\downarrow 0.2291
115	IPI00000105.4	MVP, major vault protein	\downarrow 0.2377
116	IPI00027720.1	PNLIP, pancreatic triacylglycerol lipase precursor	\downarrow 0.2421
117	IPI00140420.4	SND1	\downarrow 0.2805
118	IPI00515061.3	HIST1H2BJ, histone H2B type 1-J	\downarrow 0.2884
119	IPI00410714.5	HBA1, hemoglobin subunit α	\downarrow 0.2911
120	IPI00295663.1	ELA3A, elastase-3A precursor	\downarrow 0.2965
121	IPI00298497.3	FGB, fibrinogen β chain precursor	\downarrow 0.2992
122	IPI00759832.1	YWHAB, isoform short of 14-3-3 protein β/α	\downarrow 0.3020
123	IPI00003527.5	SLC9A3R1	\downarrow 0.3221
124	IPI00788782.1	ATP1A3, Na ⁺ /K ⁺ -ATPase α 3 subunit variant	\downarrow 0.3404
125	IPI00028908.3	NID2, nidogen-2 precursor	\downarrow 0.3532
126	IPI00186290.6	EEF2, elongation factor 2	\downarrow 0.3698
127	IPI00010779.4	TPM4, isoform 1 of tropomyosin α -4 chain	\downarrow 0.3767
128	IPI00873444.1	UBC, RPS27A 79 kDa protein	\downarrow 0.3837
129	IPI00156689.3	VAT1	\downarrow 0.3945
130	IPI00178926.2	IGJ, immunoglobulin J chain	\downarrow 0.3981
131	IPI00021827.3	DEFA3, neutrophil defensin 3 precursor	\downarrow 0.3981
132	IPI00337741.4	APEH, acylamino-acid-releasing enzyme	\downarrow 0.4055
133	IPI00292530.1	ITIH1, inter- α -trypsin inhibitor heavy chain H1	\downarrow 0.4169
134	IPI00031522.2	HADHA, trifunctional enzyme subunit α	\downarrow 0.4207
135	IPI00426051.3	Putative uncharacterized protein DKFZp686C15213	\downarrow 0.4246
136	IPI00009027.1	REG1A, lithostathine-1- α precursor	\downarrow 0.4246
137	IPI00300725.7	KRT6A, type II cytoskeletal 6A	\downarrow 0.4365
138	IPI00555744.6	RPL14 protein	\downarrow 0.4529
139	IPI00465361.4	RPL13, 60S ribosomal protein L13	\downarrow 0.4571
140	IPI00843810.2	CEL, carboxyl ester lipase	\downarrow 0.4699
141	IPI00024933.3	RPL12, 60S ribosomal protein L12	\downarrow 0.4966
142	IPI00845263.1	FN1, fibronectin 1 isoform 2 preproprotein	\downarrow 0.5012
143	IPI00449920.1	IGHA1, highly similar to Ig α -1 chain C region	\downarrow 0.5105
144	IPI00289862.3	SCRN1, secernin-1	\downarrow 0.5105
145	IPI00002745.1	CTS2, cathepsin Z precursor	\downarrow 0.5152
146	IPI00005924.4	PNLIPRP2, pancreatic lipase-related protein 2	\downarrow 0.5297
147	IPI00873137.1	COL1A2, 130 kDa protein	\downarrow 0.5346
148	IPI00783512.1	Reversed PTPRN2 110 kDa protein	\downarrow 0.5346
149	IPI00552768.1	TXN, thioredoxin	\downarrow 0.5346
150	IPI00294380.5	PCK2	\downarrow 0.5395
151	IPI00007765.5	HSPA9, stress-70 protein, mitochondrial precursor	\downarrow 0.5445
152	IPI00472724.1	EEF1AL3, elongation factor 1- α -like 3	\downarrow 0.5495
153	IPI00297646.4	COL1A1, collagen α -1(I) chain	\downarrow 0.5495
154	IPI00307162.2	VCL, isoform 2 of vinculin	\downarrow 0.5649
155	IPI00009826.2	CPB1, carboxypeptidase B precursor	\downarrow 0.5649
156	IPI00003362.2	HSPA5 protein	\downarrow 0.5649

Table II. Continued.

No.	Accession no.	Protein name	GMAH vs. NGM
157	IPI00305461.2	ITIH2, inter- α -trypsin inhibitor heavy chain H2	↓0.5754
158	IPI00027497.5	GPI, glucose-6-phosphate isomerase	↓0.5971
159	IPI00061005.4	ERP27, endoplasmic reticulum-resident protein ERp27	↓0.6138
160	IPI00298994.6	TLN1, talin-1	↓0.6194
161	IPI00026302.3	RPL31, 60S ribosomal protein L31	↓0.6194
162	IPI00856098.1	p180/ribosome receptor	↓0.6252
163	IPI00216134.3	TPM1, tropomyosin 1 α chain isoform 7	↓0.6252
164	IPI00009823.3	CPA1, carboxypeptidase A1 precursor	↓0.6486
165	IPI00009867.3	KRT5, type II cytoskeletal 5	↓0.6607

S100A6 and SOD3 are highlighted in bold. NGM, normal gastric mucosa; GMAH, gastric mucosal atypical hyperplasia; ↑, upregulation of expression in GMAH mesenchyma; ↓, downregulation of expression in GMAH mesenchyma.

Table III. Expression levels of S100A6 and SOD3 proteins in the NGM and GMAH tissues.

Protein	n	Score			Positive rate, %
		Low (-)	Moderate (+)	High (+++)	
SOD3					
NGM	20	8	8	4	60.00
GMAH	20	14	4	2	30.00 ^a
S100A6					
NGM	20	13	4	3	35.00
GMAH	20	7	11	2	65.00 ^a

^aP<0.05, GMAH vs. NGM tissues. SOD3, superoxide dismutase 3; S100A6, S100 calcium-binding protein A6; NGM, normal gastric mucosa; GMAH, gastric mucosal atypical hyperplasia.

expression of S100A6 and SOD3 was analyzed by western blotting and immunohistochemical staining techniques, and was identified to be significantly different and associated with tumorigenesis. These results were consistent with the results of quantitative proteomics in the present study.

S100A6 is a member of the S100 protein family (15). S100A6 has a number of biological functions, including participating in the degradation and ubiquitination of β -catenin, promoting apoptosis, interacting with extracellular matrix proteins, enhancing cell metabolism and skeleton depolymerization, participating in endocytosis and exocytosis, adjusting enzyme activity, inhibiting protein kinase C-mediated phosphorylation and participating in gene transcription (16,17). A number of studies have demonstrated that S100A6 is also associated with the occurrence and development of tumors and is upregulated in several tumors, including ovarian cancer, colorectal cancer, pancreatic cancer, liver cancer, malignant melanoma and osteosarcoma (18,19). According to the results of the present study, S100A6 is upregulated in the GMAH stroma. This protein may contribute to the malignant transformation of epithelial cells of gastric mucosa and promote cell invasion and metastasis. The S100A6 protein

may be a potential biomarker for monitoring malignant cell transformation.

Mammalian SODs have three subtypes, namely the cytoplasmic SOD (CuZnSOD or SOD1), mitochondrial SOD (MnSOD or SOD2) and extracellular SOD (EC-SOD or SOD3) (20). SOD3 serves an important function in maintaining the oxidation balance that prevents nuclear DNA and protein oxidative damage in the extracellular matrix and nucleus (21). Previous studies have identified that the level of SOD3 was decreased in a variety of tumors, including lung, breast and thyroid cancer, and renal cell carcinoma (10,22). SOD3 is widely expressed in normal tissues; low or no expression of SOD3 causes an imbalance in the extracellular redox environment and cancer occurs more frequently in an imbalanced environment (23). Therefore, a low or no expression of SOD3 may be a risk factor for malignant cell transformation (24). The results of the present study demonstrated that SOD3 was downregulated in GMAH stroma, which resulted in DNA damage in gastric mucosa epithelial cells and GC. Therefore, the early detection of SOD3 may predict the occurrence of GC.

As the tumor microenvironment serves a critical function in GC occurrence and development, it important to identify

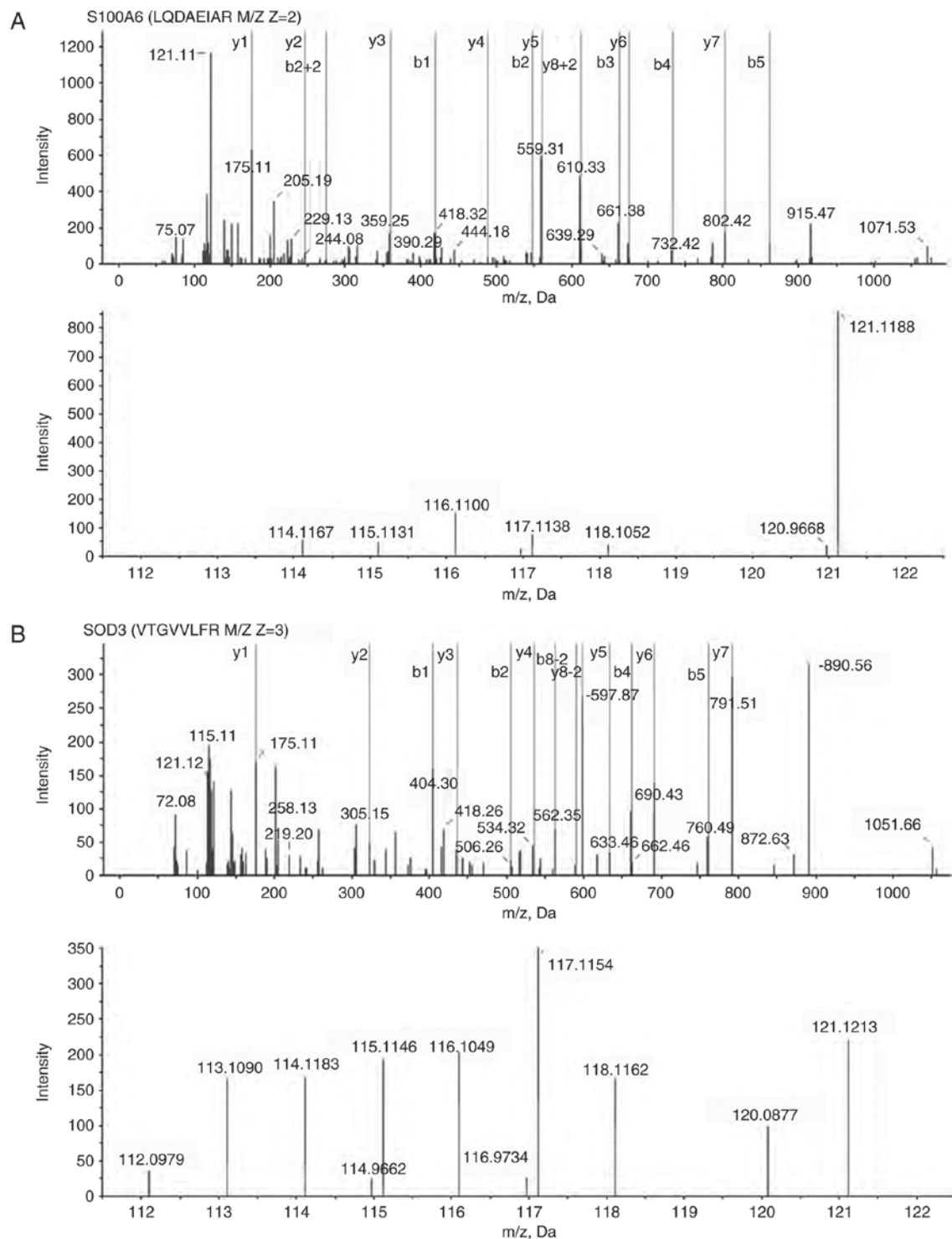


Figure 2. Mass spectrometry and quantification of S100A6 and SOD3 proteins. (A) Top: The peptide mass fingerprint and sequence LQDAEIAR allowed the identification of S100A6. Bottom: The released iTRAQ reporter ions provided the relative quantification of S100A6 from the mesenchyma of NGM and GMAH tissues evaluated. (B) Top: The peptide mass fingerprint and sequence VTGVVLF allowed the identification of SOD3. Bottom: The released iTRAQ reporter ions provide the relative quantification of SOD3 from the two tissues evaluated. S100A6, S100 calcium-binding protein A6; SOD3, superoxide dismutase 3; iTRAQ, isobaric tags for relative and absolute quantitation.

the proteins present in the GMAH microenvironment. The present study identified a total of 165 differentially expressed proteins in GMAH stroma. These data will further clarify the molecular mechanisms of GC occurrence as well as potentially serving as prognostic markers for the early detection and diagnosis of GC.

Acknowledgements

The authors would like to thank Dr Qiang Zhao from The First Affiliated Hospital of University of South China (Hengyang, China) for his help in collecting specimens. The authors would also like to thank Professor Zhao-Yang Luo

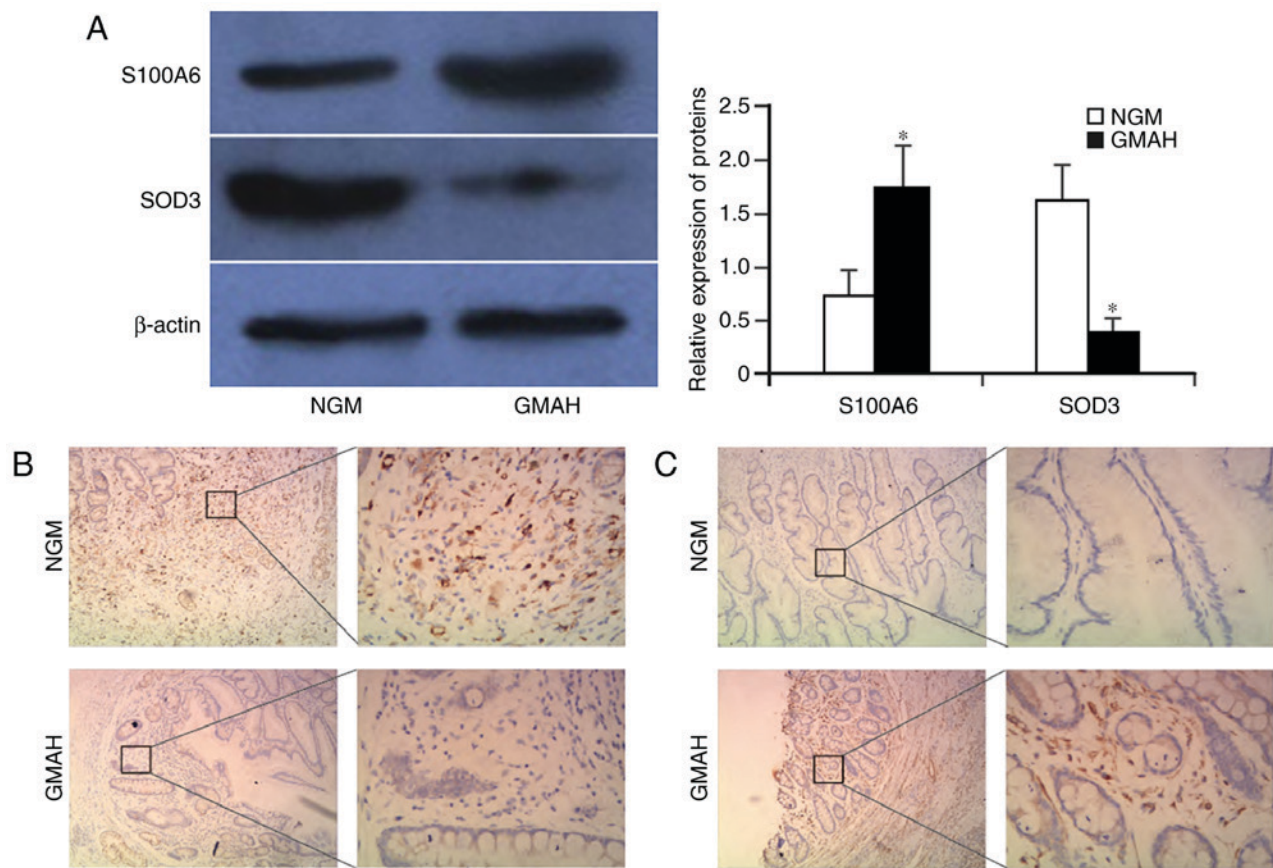


Figure 3. Expression of S100A6 and SOD3 proteins in the mesenchyma of NGM and GMAH tissues. (A) The expression of S100A6 and SOD3 proteins in NGM and GMAH mesenchymal tissues were detected by western blot analysis. Expression levels of proteins in two tissues were determined by densitometric analysis (n=3; *P<0.01 vs. NGM). (B) Immunohistochemistry revealed the expression of the S100A6 protein in NGM and GMAH mesenchyma. Original magnification, x10 (left) and x40 (right). (C) Immunohistochemistry revealed the expression of the SOD3 protein in NGM and GMAH mesenchyma. Original magnification, x10 (left) and x40 (right). S100A6, S100 calcium-binding protein A6; SOD3, superoxide dismutase 3; NGM, normal gastric mucosa; GMAH, gastric mucosal atypical hyperplasia.

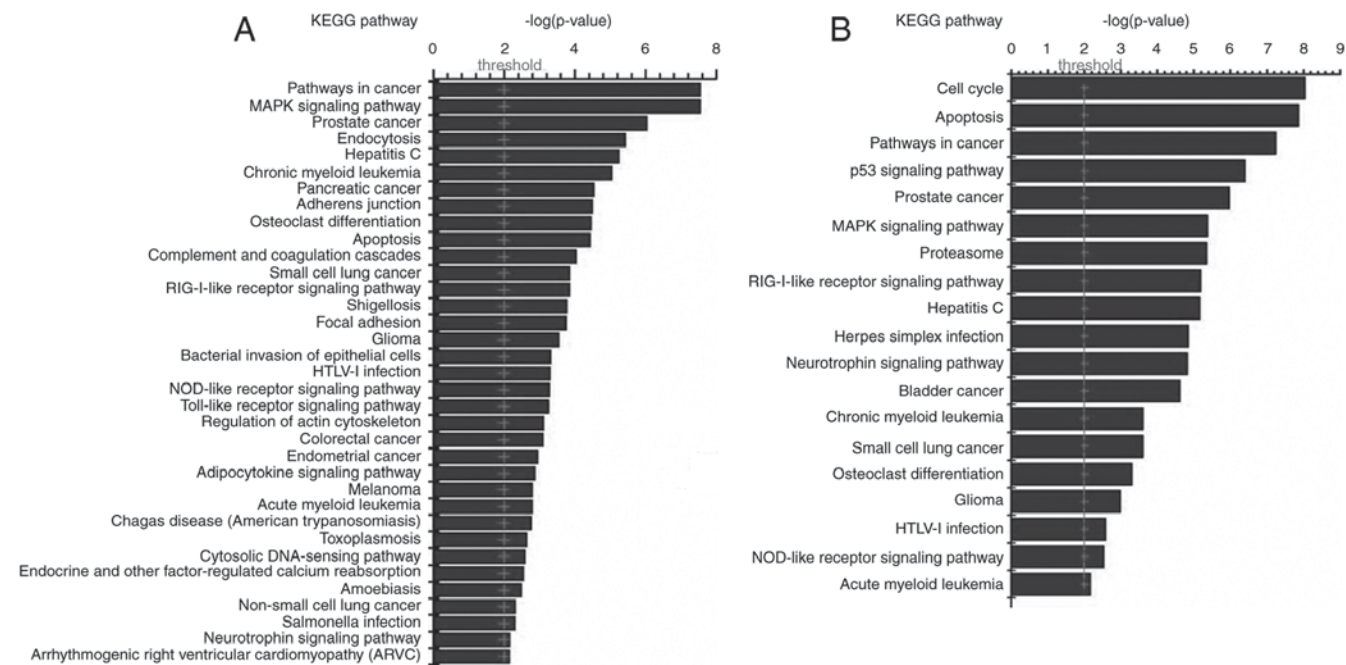


Figure 4. KEGG signal pathway analysis of differentially expressed proteins analyzed using Cytoscape software. (A) The signal pathway involved in the proteins that are upregulated in GMAH compared with NGM tissues. (B) The signal pathway involved in the proteins that are downregulated in GMAH compared with NGM tissues. KEGG, Kyoto Encyclopedia of Genes and Genomes; NGM, normal gastric mucosa; GMAH, gastric mucosal atypical hyperplasia; MAPK, mitogen-activated protein kinase; RIG, retinoic acid-induced gene; HTLV, human T-lymphotropic virus; NOD, nucleotide-binding oligomerization domain.

and Professor Xiu-Tian Zhou from the Cancer Research Institute of the University of South China (Hengyang, China) for their assistance in the diagnosis of specimens.

Funding

The present study was supported by the Hunan Provincial Innovation Foundation For Postgraduates (grant no. CX2016B478), the Doctoral Research Start-Up Fund of the University of South China (grant no. 2016XQD21), the Hunan Provincial Groundbreaking Platform Open Fund of the University of China (grant no. 10K052, 12K094 and 13K083), the Hunan Provincial Education Department Foundation of China (grant nos. 11C1112 and 12C0340), the Hunan Provincial Health Department Foundation of China (grant nos. B2013-048 and 2014-163) and the Construct Program of the Key Discipline in Hunan Province of China (2011-76).

Availability of data and materials

All data generated or analyzed during this study are included in this published article.

Authors' contributions

ZWZ and CYL conceived and designed the experiments. HLZ, WM and CJL performed the experiments. LH and CSL analyzed the data. HLZ and ZWZ wrote the paper. All authors read and approved the manuscript.

Ethics approval and consent to participate

All patients involved in this study provided written informed consent, and the present study was approved by the Medical Ethics Committee of University of South China. Written informed consent was obtained from all participants.

Consent for publication

All patients provided their written informed consent for the publication of their data.

Competing interests

The authors declare that they have no conflicts of interest.

References

- Chen W, Zheng R, Baade PD, Zhang S, Zeng H, Bray F, Jemal A, Yu XQ and He J: Cancer statistics in China, 2015. *CA Cancer J Clin* 66: 115-132, 2016.
- Lim B, Kim JH, Kim M and Kim SY: Genomic and epigenomic heterogeneity in molecular subtypes of gastric cancer. *World J Gastroenterol* 22: 1190-1201, 2016.
- Correa P: Human gastric carcinogenesis: A multistep and multifactorial process-First American Cancer Society Award lecture on cancer epidemiology and prevention. *Cancer Res* 52: 6735-6740, 1992.
- Kohlhapp FJ, Mitra AK, Lengyel E and Peter ME: MicroRNAs as mediators and communicators between cancer cells and the tumor microenvironment. *Oncogene* 34: 5857-5868, 2015.
- Rodvold JJ and Zanetti M: Tumor microenvironment on the move and the Aselli connection. *Sci Signal* 9: fs13, 2016.
- Langley RR and Fidler IJ: The seed and soil hypothesis revisited-the role of tumor-stroma interactions in metastasis to different organs. *Int J Cancer* 128: 2527-2535, 2011.
- Chin AR and Wang SE: Cancer tills the premetastatic field: Mechanistic basis and clinical implications. *Clin Cancer Res* 22: 3725-3733, 2016.
- Amin MB, Edge SB, Greene FL, Byrd DR, Brookland RK, Washington MK, Gershenwald JE, Compton CC, Hess KR, Sullivan DC, *et al*: *AJCC cancer staging manual*. 8th ed. New York: Springer 203-220, 2016.
- Wang XH, Du H, Li L, Shao DF, Zhong XY, Hu Y, Liu YQ, Xing XF, Cheng XJ, Guo T, *et al*: Increased expression of S100A6 promotes cell proliferation in gastric cancer cells. *Oncol Lett* 13: 222-230, 2017.
- Kim J, Mizokami A, Shin M, Izumi K, Konaka H, Kadono Y, Kitagawa Y, Keller ET, Zhang J and Namiki M: SOD3 acts as a tumor suppressor in PC-3 prostate cancer cells via hydrogen peroxide accumulation. *Anticancer Res* 34: 2821-2831, 2014.
- Yan M and Jurasz P: The role of platelets in the tumor microenvironment: From solid tumors to leukemia. *Biochim Biophys Acta* 1863: 392-400, 2016.
- Justus CR, Sanderlin EJ and Yang LV: Molecular connections between cancer cell metabolism and the tumor microenvironment. *Int J Mol Sci* 16: 11055-11086, 2015.
- Linton SS, Sherwood SG, Drews KC and Kester M: Targeting cancer cells in the tumor microenvironment: Opportunities and challenges in combinatorial nanomedicine. *Wiley Interdiscip Rev Nanomed Nanobiotechnol* 8: 208-222, 2016.
- Wu AA, Drake V, Huang HS, Chiu S and Zheng L: Reprogramming the tumor microenvironment: Tumor-induced immunosuppressive factors paralyze T cells. *Oncoimmunology* 4: e1016700, 2015.
- Schneider G and Filipek A: S100A6 binding protein and Siah-1 interacting protein (CacyBP/SIP): Spotlight on properties and cellular function. *Amino Acids* 41: 773-780, 2011.
- Leśniak W, Słomnicki ŁP and Filipek A: S100A6-new facts and features. *Biochem Biophys Res Commun* 390: 1087-1092, 2009.
- Kasacka I, Piotrowska Ż, Filipek A and Majewski M: Influence of doxazosin on biosynthesis of S100A6 and atrial natriuretic factor peptides in the heart of spontaneously hypertensive rats. *Exp Biol Med (Maywood)* 241: 375-381, 2016.
- Zhang J, Zhang K, Jiang X and Zhang J: S100A6 as a potential serum prognostic biomarker and therapeutic target in gastric cancer. *Dig Dis Sci* 59: 2136-2144, 2014.
- Duan L, Wu R, Zou Z, Wang H, Ye L, Li H, Yuan S, Li X, Zha H, Sun H, *et al*: S100A6 stimulates proliferation and migration of colorectal carcinoma cells through activation of the MAPK pathways. *Int J Oncol* 44: 781-790, 2014.
- Che M, Wang R, Li X, Wang HY and Zheng XFS: Expanding roles of superoxide dismutases in cell regulation and cancer. *Drug Discov Today* 21: 143-149, 2016.
- Wang YD, Chen WD, Li C, Guo C, Li Y, Qi H, Shen H, Kong J, Long X, Yuan F, *et al*: Farnesoid X receptor antagonizes JNK signaling pathway in liver carcinogenesis by activating SOD3. *Mol Endocrinol* 29: 322-331, 2015.
- Xu D, Li Y, Li X, Wei LL, Pan Z, Jiang TT, Chen ZL, Wang C, Cao WM, Zhang X, *et al*: Serum protein S100A9, SOD3, and MMP9 as new diagnostic biomarkers for pulmonary tuberculosis by iTRAQ-coupled two-dimensional LC-MS/MS. *Proteomics* 15: 58-67, 2015.
- Griess B, Tom E, Domann F and Teoh-Fitzgerald M: Extracellular superoxide dismutase and its role in cancer. *Free Radic Biol Med* 112: 464-479, 2017.
- O'Leary BR, Fath MA, Bellizzi AM, Hrabe JE, Button AM, Allen BG, Case AJ, Altekruze S, Wagner BA, Buettner GR, *et al*: Loss of SOD3 (EcSOD) expression promotes an aggressive phenotype in human pancreatic ductal adenocarcinoma. *Clin Cancer Res* 21: 1741-1751, 2015.



This work is licensed under a Creative Commons Attribution-NonCommercial-NoDerivatives 4.0 International (CC BY-NC-ND 4.0) License.